

Securing Iris Recognition System for Access Control Based on Image Processing

Isaack Adidas Kamanga¹, Dening Jiang²

¹Tianjin University of Technology and Education, Tianjin, China, P.R
Electronic Engineering Department

²Professor, Tianjin University of Technology and Education, Tianjin, China, P.R
Electronic Engineering Department

Abstract: Results of different studies show that iris recognition is a viable, fast, and easy way to authenticate a person's identity and it is the most accurate biometric approach for authentication. The findings are so positive that the prospect of iris prints replacing PINs and other identification methods is much more viable, new studies found that an eye from a dead person would deteriorate too fast to be useful, so no extra precautions have to be taken to be sure the user is a living human being. The big challenge with iris recognition is that an iris scanning security can be cheated by presenting a high resolution still image of an eye to the iris scanner instead of a live eye, also can be cheated by using video frames and 3D model of valid individual. With increasing e-payments nowadays, Un supervised passages with iris scan as a security, a hack-able security can assists criminals and others to access personal and financial information of an individual and in turn, the loss of trust, confidence and respect. This research work propose a more secured iris recognition system which incorporate the ability to detect the aliveness of the individual being scanned by the system for identification to prevent possible spoofing using photographs, videos, and 3D models of a valid user. An algorithm has been developed adapting a proposed improved canny edge detection method, this algorithm validates the user being scanned by three stages which are; Eye blink detection, Background subtraction and correlation, and Straight line border edge detection. All these three stages are performed using digital image processing techniques

Keywords: Biometric ID, Iris recognition, Hamming distance, Eye blink, IrisCode

1. Introduction

With technology growing and taking a new face, a demand for more secure and viable authentication technique is inevitable. Traditional techniques like passwords, pins, tokens, bar code etc can be forgotten, stolen or duplicated easily. A biometric technology is playing a celebrate-able role in accuracy and reliability, out of a number of biometric security systems such as; facial recognition, voice recognition, signature recognition, DNA, retina scanning, Iris recognition, finger print [2] and hand geometry and now research is going on ear structure[13], Iris recognition is the most secure and accurate method for authentication, Daugman found that the chance of iris patterns from two individuals to be similar is almost impossible[14], therefore iris pattern is ideal label for authentication, it actually supersede finger print ID because of the fact that even a finger print of a dead person can be used to authenticate whilst it has been found that immediate after death the structure of the iris pattern changes and therefore impossible to authenticate[13]

Biometric ID- is a distinctive, measurable characteristic that can be used to label and describe the uniqueness of individual [17] such as iris patterns, finger prints, facial recognition etc, generally There are two main types of biometric identifiers; Physiological characteristics(The shape or composition of the body such as DNA, face , finger prints, hand geometry, retina or Iris patterns) and Behavioral characteristics (The behavior of a person such as typing rhythm, gait, gestures and voice)[17]. Other areas that are being researched in the quest to improve biometric authentication include brainwave signals, and a password pill

that contains a microchip powered by the acid present in the stomach. Once swallowed, it creates a unique ID radio signal that can be sensed from outside the skin, turning the entire body into a password. Authentication by biometric verification is becoming increasingly common in corporate and public security systems, consumer electronics, and point-of-sale applications. In addition to security, the driving force behind biometric verification has been convenience, as there are no passwords to remember or security tokens to carry [17].

Why Biometric ID-The key reason to as why we need Biometric identification is because the ID cannot be forgotten, not easily copied, versatile and reduce the burden of carrying along, things like security/bank cards, passports etc which can easily be forgotten at home.

Iris Recognition- Is the process of recognizing a person by taking a picture of an eye analyzing the random patterns of the iris [18]. The automated method of iris recognition is relatively modern, existing in patent only since 1990s [18].The iris is a muscle within the eye that regulates the size of the pupil (figure 1 (a)), controlling the amount of light that enters the eye. It is the colored portion of the eye with coloring based on the amount of melanin pigment within the muscle [17], the iris of human eye is the annular part between the black pupil and white sclera. It is located behind the cornea, iris is the only internal organ that is usually externally visible, the diameter of iris is only 12mm but it has a highly complex structure. Under infrared illumination, iris displays rich texture determined by many distinctive minutes. Such iris texture is distinctive between persons and stable

over individual's life time, which makes iris particularly useful for personal identification.

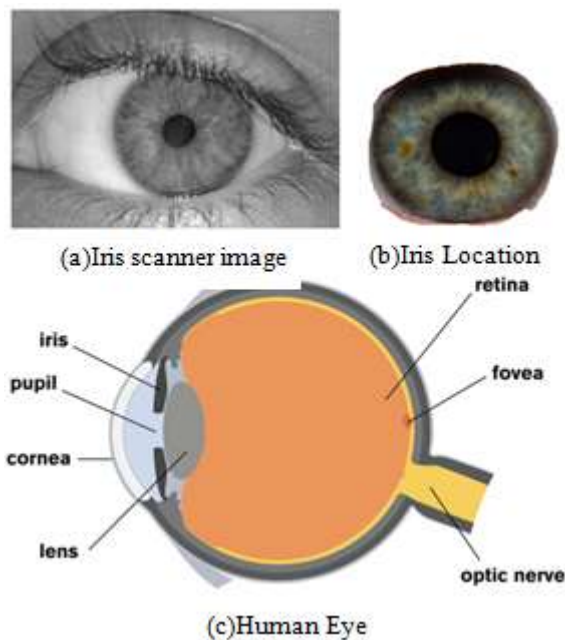


Figure 1: (a) Image from Iris Scan Model 2100 camera (b) Location of an iris and (c) Human Eye

2. Proposed Model with Antispoof

2.1 Image Acquisition

Iris recognition system works by first a scanner taking a picture of an eye (figure 1(a)) when an eye is illuminated with near infrared light in the 700–900-nm band (used in all current iris scanning cameras), even dark brown irises reveal rich texture[19], the existing system is able to take the picture from a printed still picture with high resolution like 1200x1200 dpi, providing a window for bypassing a security check by presenting the image of another person, the proposed model comprises the additional hardware but utilizing the same infra red radiation to confirm whether the image being taken is the living eye of from a picture or dead person. Once image of the eye is taken the software convert it to gray scale locates the iris within the image then the image is enhanced for further processing. Segmentation and later normalization follows (these are discussed in detail bellow). The normalized and dimensionless iris mapping is encoded into an IrisCode through a process of demodulation that extracts phase sequences, Gabor wavelets transform is used in order to extract the spatial frequency range that contains a good best signal-to noise ratio considering the focus quality of available cameras. The result is a set of complex numbers that carry local amplitude and phase information for the iris image called the IrisCode [19].

111001010100
 001010101001
 010001001010

Figure 2: An example of Iris Signature

Before any further processing of the acquired iris image, this model works by first employing an algorithm to verify that there is no a spoof attempt.

2.1.1 Antispoof algorithm design

The combined effect of this algorithm is the ability to detect eye blink, detecting high background correlation between stored background and current acquired one from a video frame and finally the ability to find border edge line which is the sign of photograph spoofing

2.1.2 Detecting eye blink

Blinking is a semi-autonomic rapid closing of the eyelid. A single blink is determined by the forceful closing of the eyelid or inactivation of the levator palpebrae superioris and the activation of the palpebral portion of the orbicularis oculi, not the full open and close [8]. A blink lasts about a 10th of a second, and most people blink about 15 times a minute, or every 4 seconds. Eye blink in general lasts from 150 to 300ms [8]. To achieve eye blink detection, a flowchart bellow is engaged

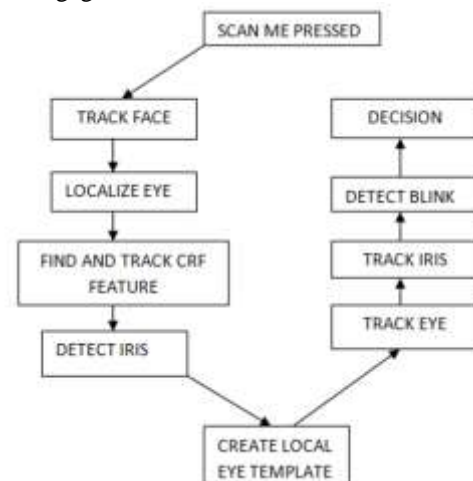


Figure 3: Blink detection flowchart

The Viola-Jones face detector is employed which uses Haar feature-based cascade classifiers with two stages as in figure 4 bellow. In face detection initially, the algorithm needs a lot of positive images (images of faces) and negative images (images without faces) to train the classifier as detailed in [8] and [9]. After detecting the face, CRT features are used to track the face.

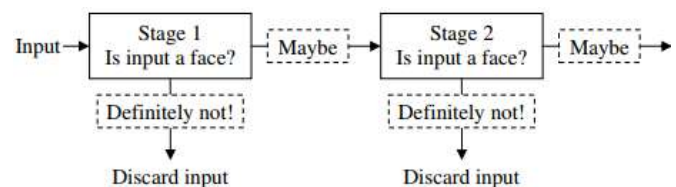


Figure 4: The cascaded classifier

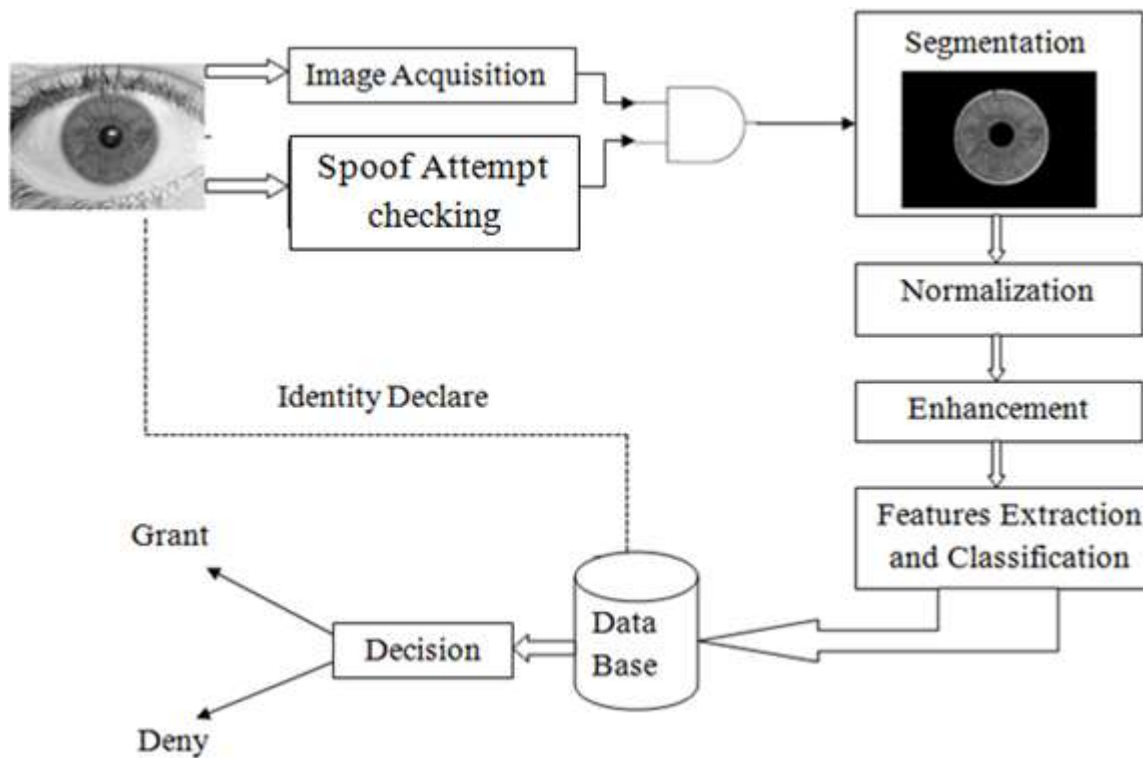


Figure 5: Proposed model block diagram

2.1.2.1 CRF Feature tracking

Conditional Random Fields shortened as CRF features Are classes of statistical modeling methods applied in pattern recognition and machine learning and used for structured prediction [16]. CRFs are type of discriminative undirected probabilistic graphical model. Are used to encode known relationships between observations and construct consistent interpretations, in computer vision; CRFs are often used for object recognition and image segmentation [19].

To super pass the effect that could be brought by slight movement of the head, a feature that is unique and robust should be selected as a reference point for tracking to compensate for minor head movements. These facial features could be point features (eye corners), edge features (lip contours) or texture features (skin color). In this work I choose CRF features due to their discriminative nature. The typical eye states are *opening* and *closing* suppose that S is a random variable over observation sequences to be labeled and Y is a random variable over the corresponding label sequences to be predicted. All of components y_i of Y are assumed to range over a finite label set Q . Using the Hamersley and Clifford theorem, the joint distribution over the label sequence Y given the observation S can be written as the following form

$$P_{\theta}(Y/S) = \frac{1}{Z_{\theta}(S)} \exp \left(\sum_{t=1}^T \Psi_{\theta}(Y_t, Y_{t-1}, S) \right) \quad (1)$$

Given that $Z_{\theta}(S)$ is a normalized factor summing over all state sequences and an exponentially large number of terms

$$Z_{\theta}(S) = \sum_Y \exp \left(\sum_{t=1}^T \Psi_{\theta}(Y_t, Y_{t-1}, S) \right) \quad (2)$$

The potential function $\Psi_{\theta}(Y_t, Y_{t-1}, S)$ is the sum of CRF features at time t :

$$\Psi_{\theta}(Y_t, Y_{t-1}, S) = \sum_i \lambda_i f_i(Y_t, Y_{t-1}, S) + \sum_j \mu_j g_j(Y_t, S) \quad (3)$$

Where by $\theta = \{\lambda_1, \dots, \lambda_A; \mu_1, \dots, \mu_B\}$, to be estimated from training data.

The *within-label* feature functions f_i are as:

$$f_i(Y_t, Y_{t-1}, S) = 1\{y_t = l\} 1\{y_{t-1} = l'\} \quad (4)$$

The *between-observation-label* feature functions g_j are as:

$$g_j(Y_t, S) = 1_{\{y_t=l\}} U(I_{t-w}) \quad (5)$$

Where $l \in Q$, $w \in [-W, W]$, and $U(I)$ is *eye closity*, *eye closity*, $U(I)$, measuring the degree of eye's closeness

$$U_M(I) = \sum_{i=1}^M \left(\log \frac{1}{\beta_i} \right) h_i(I) - \frac{1}{2} \sum_{i=1}^M \log \frac{1}{\beta_i} \quad (6)$$

Where, $\beta_i = \frac{1}{2}(1 - \frac{1}{2})$ (7) and $h_i(I) : \text{RDim}(I) \rightarrow \{0, 1\}$, $i = 1, \dots, M$ is a set of binary weak classifiers

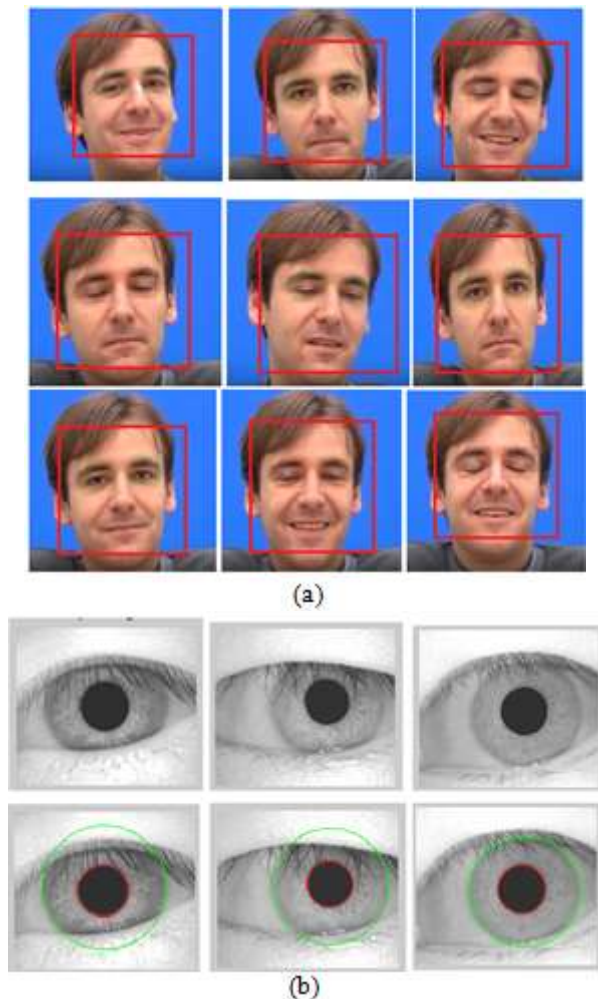


Figure 6: (a) Detected faces and tracking, testing made on Talking face database and (b) located irises, CASIA database (eye images and the corresponding images showing detected irises and pupils bounding the region of interest)

2.1.2.2 Creating local eye template

The eye region located is fairly larger than the actual eye. Thus the user should be allowed limited head motion as long as the eye remains within this region. When the user is required to look at the centre of the screen as a part of the training procedure, an eye template is extracted based on the iris position and size.. This eye template is typically smaller than the eye region and allows the user some freedom to move around slightly. It serves to restrict the region of the eye image that is searched in order to detect the iris or evaluate a blink, thus reducing errors and unnecessary processing. After localizing the eye we need to track it and the iris too.

Local eye tracking using normalized cross correlation. An eye tracking procedure maintains exact knowledge about the eye's appearance. In order to track the template, the system utilizes the normalized correlation coefficient R proposed by [8][9] as follows

$$R(x, y) = \frac{\sum_{y'=0}^h \sum_{x'=0}^w T(x', y') I(x+x', y+y')}{\sqrt{\sum_{y'=0}^h \sum_{x'=0}^w T(x', y')^2 \sum_{y'=0}^h \sum_{x'=0}^w I(x+x', y+y')^2}} \quad (7)$$

where $T(x', y') = T(x', y') - T^-$, $I(x+x', y+y') = I(x+x', y+y') - I^-(x, y)$ and $T(x, y)$ and $I(x, y)$ are the brightness of the pixels at (x, y) in the template and source image, respectively, and T^- is the average value of the pixels in the template raster and $I^-(x, y)$ is the average value of the pixels in the current search window of the image. The coefficient $R(x, y)$ is a measure of the match between the open eye template and all points within the small search region surrounding the location of the eye given from the previous frame

2.1.2.3 Detect Blink

Now as we have the local template and we are tracking the eye in real time, the next step is to detect an eye blink. In this work a method proposed by [16], blink detection by motion variant is implemented in MATLAB for blink detection. We focus on detection of an individual eye blinks before passing the program counter to continue with recognition steps like segmentation normalization etc and finally grant or deny access to an individual. Partial closed eye is called an incomplete blink and in this case is considered to as a NOT A BLINK. Eye blink in general lasts from 150 to 300ms [17]. Thus a standard camera with 25 / 30 frames per second like one in our mobile phones is sufficient for eye blink monitoring. The region of interest is divided into halves to separate individual eye regions. The method runs separately for each eye. A flock of KLT trackers is placed over a regular grid (Fig. 1) spaced with 1/15 of the region dimensions (all together around 225 trackers, that count depends on the region size). Next, local motion vectors are extracted and averaged based on their locations. An average variance of vertical components of the 6 upper motion vectors is the input to a state machine, which detects an eye blink

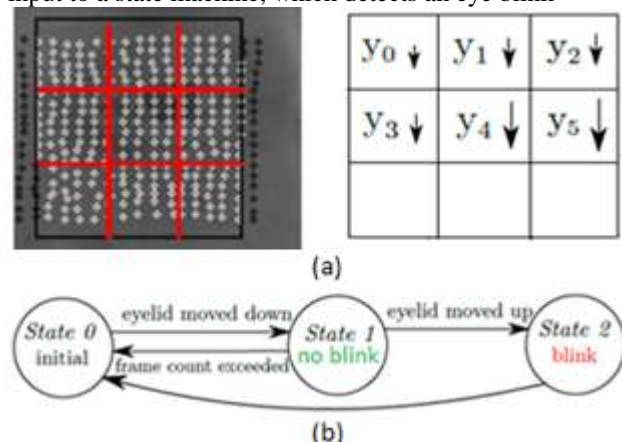


Figure 7: (a) The gray dots representing the trackers used to calculate the motion vectors and (b) state machine of eye blink detection

Kanade-Lucas-Tomasi (KLT) feature tracker is an approach to feature extraction. It is proposed mainly for the purpose of dealing with the problem that traditional image registration techniques are generally costly. KLT makes use of spatial intensity information to direct the search for the position that yields the best match. It is faster than traditional techniques for examining far fewer potential matches between the images [14]. You can find the detail of this algorithm in [14]. The region is divided into 9 cells (Fig. 7 (a)). An average cell motion vector is calculated for a cell from the individual local motion vectors belonging to the cell based on their locations. Eye blink causes a significant

vertical move in the cells of middle row, but only a minor move in the top or bottom row. Motion vectors have different characteristics during head movements or other facial mimics. The vertical components of the middle and top rows are sufficient for further computation. From these 6 (y_0 - y_6) motion vectors the variance $\text{var}(y)$ (Eqn 8) is calculated

$$\mu = \frac{\sum_i y_i}{6}, \quad \text{Var}(y) = \frac{\sum_i (\mu - y_i)^2}{6} \quad (8)$$

Statistical variance of the 6 upper cells represents the diversity across moves. If the variance is higher than the variance threshold T_v , it will indicate an eyelid has moved.

Variance is invariant to position changes of the person's face, and therefore no head movement compensation is necessary. The variance threshold is evaluated empirically on our dataset as

$$T_v = kx \frac{d}{fps} \quad (9)$$

Where by:

k : is a constant value is 0.018. based on testing

d : The interocular distance (depends on separation between individual and camera)

fps : The frame rate of the input video from databases used (Taking Face)

I used the publicly available ZJU databases for testing on how many blinks I count and miss, also calculated the efficiency of this approach which is higher than the landmark based approach suggested by [8].

2.1.3 Background Subtraction and comparing

As enlightened by [25][26][28], background subtraction, also known as foreground detection, is a technique in the fields of image processing and computer vision wherein an image's foreground is extracted for further processing (object recognition etc.). Background subtraction is a widely used approach for detecting moving objects in videos from static cameras, in this work it is used for detecting any change in the background which under no spoofing scenario, no background changes are expected. The implementation follows the flowchart below

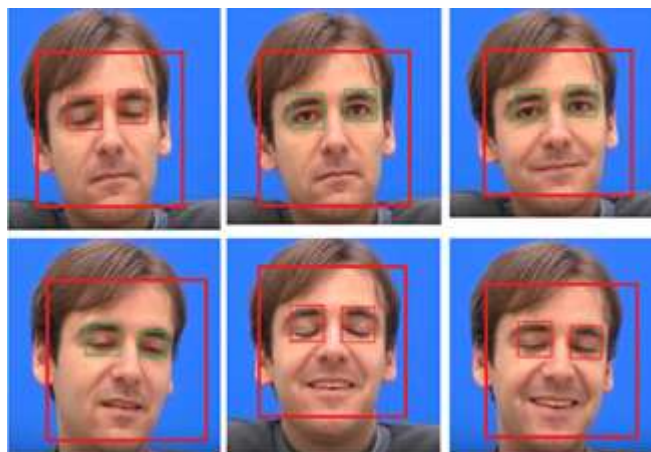


Figure 8: Detected blinks and ne blink miss by the algorithm

Blinks are indicated by red bouncing box while open eye

state indicated by green bouncing boxes, face is continuously tracked by a red bouncing box

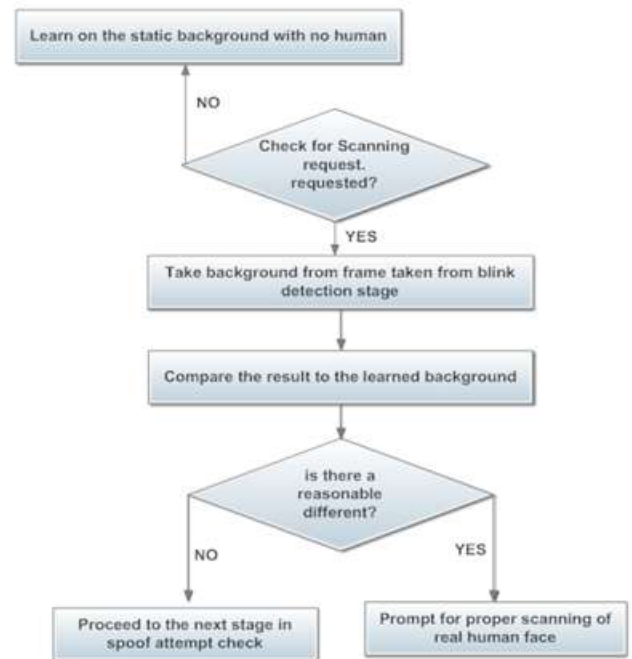


Figure 9: Background subtraction and comparison flowchart

In this work, a Background mixture models is implemented to achieve the objective. It models each pixel as a mixture of Gaussians and uses an on-line approximation to update the model. In this approach, it is assumed that every pixel's intensity values in the frame can be modeled using a Gaussian mixture model. A simple heuristic determines which intensities are most probably of the background. Then the pixels which do not match to these are called the foreground pixels. Foreground pixels are grouped using 2D connected component analysis and are of no interest at this stage.



Figure 10: Showing results of the implemented method
 Four frames of different individuals from ZJU Eyeblink database, more than 70% of the background were masked off and served for comparison, the first background was extracted an used in comparison with other frames

2.1.4 Border edge lines detection

Edge detection approach suggested by us in [19] is employed with an adaptive Gaussian filter to detect edges, see [19] for method details.

2.2 Segmentation

After spoof attempt check, the program counter is passed to next step in recognition which is segmentation. This step is performed using a variety of boundary and region detection

and active contour techniques [2]. The eyelid boundaries may be described as quadratic or cubic splines, whose parameters can be estimated by statistical model-fitting techniques. The techniques are implemented by software; here for research purpose a MATLAB algorithm has been developed for testing final result, Daugman inter deferential operator (equation 10) is adopted for localization of the iris [2][4] in this work, locating the iris is a challenge and still a research window, many approaches have been suggested like Hough Transform, Active Contour Models etc.

$$\frac{\partial}{\partial r} \left\{ \int_0^{2\pi} I(r \cdot \cos \theta + x_0, r \cdot \sin \theta + y_0) \right\} \quad (10)$$

Where (x_0, y_0) denotes the potential center of the searched circular boundary, and r is its radius.

The remapping of the iris image $I(x, y)$ from raw Cartesian coordinates (x, y) to the dimensionless non concentric polar coordinate system (r, θ) can be represented as

$$I(x(r, \theta), y(r, \theta)) \rightarrow I(r, \theta) \quad (11)$$

Where $x(r, \theta)$ and $y(r, \theta)$ are defined as linear combinations of both the set of pupillary boundary points $(x_p(\theta), y_p(\theta))$ and the set of limbus boundary points along the outer perimeter of the iris $(x_s(\theta), y_s(\theta))$ bordering the sclera[4],

$$x(r, \theta) = (1-r)x_p(\theta) + rx_s(\theta) \quad (12)$$

$$y(r, \theta) = (1-r)y_p(\theta) + ry_s(\theta) \quad (13)$$

Both of which are detected by finding the maximum of the operator (1) [4]. i.e. equation 3 below

$$\max(r, x_0, y_0) = \frac{\partial}{\partial r} \left\{ \int_0^{2\pi} I(r \cdot \cos \theta + x_0, r \cdot \sin \theta + y_0) \right\} \quad (14)$$

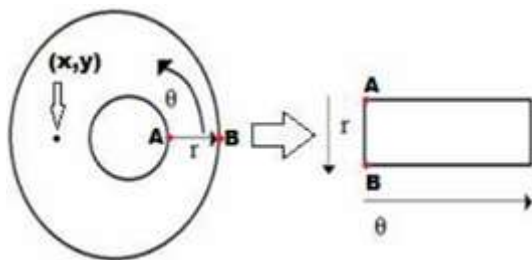


Figure 7: Polar and Cartesian coordinates of normalized eye

2.3 Normalization

After segmentation we need to prepare a segmented iris image for the feature extraction process, this process is called normalization: In Cartesian (equation 11) coordinates, iris images are highly affected by their distance and angular position with respect to the iris scanner. Moreover, illumination has a direct impact on pupil size and causes non-linear variations of the iris patterns. A proper normalization technique is expected to transform the iris image to compensate these variations. A Daugman's normalization method transforms a localized iris texture from Cartesian to polar coordinates. The proposed method is capable of

compensating the unwanted variations due to distance of eye from camera (scale) and its position with respect to the iris scanner [1][2].

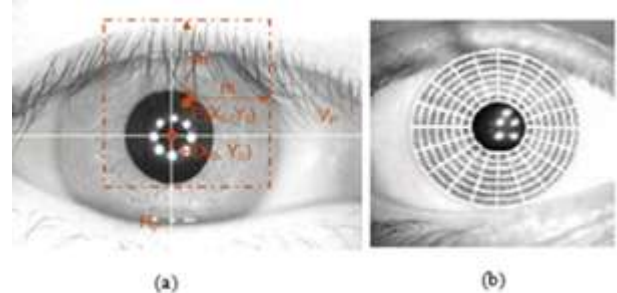


Figure 12: (a) Region of interest and (b) total number of sectors considered in this work

2.4 Enhancement

Image enhancement is a technique of predicting some of the missing details in an image such as a blurred image, to produce output(s) that is suitable for a particular application or a next stage in a given application. In the field of iris recognition, many approaches for image enhancement have been suggested, see [4] for details. Generally they are of two groups, spatial domain enhancement techniques and frequency domain enhancement techniques, this work employs a spatial domain approach called adaptive histogram equalization where by the contrast of a pixel is enhanced by equalizing the histogram of the small neighboring area, the details of this method can be read in [3][4].

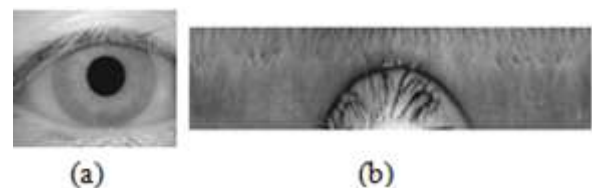


Figure 13: (a) Iris images from CASIA database and (b) a normalized image by Cartesian to polar transformation

2.5 Features Extraction using Gabor Filters

2D Gabor filter are applied to extract the iris features. A number of banks of Gabor filters are applied on images including 8 orientations

$$\theta \in \{0^0, 22.5^0, 45^0, 67.5^0, 90^0, 112.5^0, 135^0, 157.5^0\}$$

Filters, by varying the wavelengths and orientations angles of the filters [21], the result for each bank is evaluated and compared.

2.5.1 Steps in features extraction

- Locating the region of interest around the Pupil, which has been done in session 2.2 and 2.3 above
- Filtering this region in a total of eight different directions using a bank of Gabor filters (eight directions are required to completely capture the local ridge characteristics in a Iris while only four directions are required to capture the global configuration) pin pointed in [19].
- Computing the Average Absolute Deviation from the mean (AAD) of gray values in individual sectors in filtered images to define the feature vector which is the IrisCode.

2.5.1.1 Locating region of interest

Consider the gray scale image below in figure 12(a) above, Let $P(x, y)$ denote the gray level at pixel (x, y) in an $M \times N$ Iris image and let $P(X_0, Y_0)$ denote a point in pupil. The region of interest is defined as the collection of all the sectors S_i , where the i^{th} sector S_i is computed in terms of parameters (r, θ) as follows [19]

$$S_i = \{(x, y) | b(T_{i+1}) \leq r < b(T_{i+2}), \theta_i \leq \theta < \theta_{i+1}, 1 \leq x \leq N, 1 \leq y \leq M\}$$

$$T_i = \text{int}(i / k) \quad (15)$$

$$\theta_i = (i \bmod k) x (2\pi / k) \quad (16)$$

$$r = \sqrt{(x - x_0)^2 + (y - y_0)^2} \quad (17)$$

$$\theta = \tan^{-1}((y - y_0) / (x - x_0)) \quad (18)$$

Where by b represents width of each band, k is the number of sectors considered in each band, and $i = 0 \dots (B \times k - 1)$, where B is the number of concentric bands considered around the reference point for feature extraction [3][4]. For testing, CASIA images are used (image size = 256×256 pixels, scanned at 600 dpi), we considered five concentric bands ($B = 7$) for feature extraction and segmented into sixteen sectors ($k = 20$), we have a total of $20 \times 7 = 140$ sectors figure 7(b) (S_0 through S_{139}) and the region of interest is a circle of radius 60 pixels, centered at the reference point. 140 features for each of the eight filtered images provide a total of $140 \times 8 = 1120$ features per Iris image.

Filtering

A 2D Gabor filter in spatial domain is defined by equation 19 below

$$G(x, y : \theta, f) = \exp \left\{ -\frac{1}{2} \left[\frac{x'^2}{\delta x^2} + \frac{y'^2}{\delta y^2} \right] \right\} \cos(2\pi f x') \quad (19)$$

Where by

$$x' = x \cos \theta + y \sin \theta$$

$$y' = y \cos \theta - x \sin \theta$$

In equation 19 above, f is the frequency of the sinusoidal plane wave along the direction θ from x -axis, $\delta y'$ and $\delta x'$ are the space constants of the Gaussian envelope along x' and y' axes respectively. Further details of Gabor filters may be found in [3][4] also enlightened in [19].

Features vector is obtained by convolution between Gabor filter banks (8 filters one for each orientation in this case) and setting the filter frequency to the average ridge frequency ($1/k$), where k is the average inter-ridge distance. The average inter-ridge distance is approximately 6 pixels in a 600 dpi (CASIA iris database) Iris image

$$\theta \in \{0^\circ, 22.5^\circ, 45^\circ, 67.5^\circ, 90^\circ, 112.5^\circ, 135^\circ, 157.5^\circ\}$$

Each sub image is respectively filtered by these Gabor filters. This leads to a total of 1120 (8 for each sub image) output images from which the iris features are extracted.

2.5.1.2 Computing AAD

This is an average of the absolute deviations from a central

point. It is a summary statistic of statistical dispersion

Let $F_{i\theta}(x, y)$ be the filtered image for sector S_i in θ orientation and then the features value $V_{i\theta}$ is the Average absolute deviation from mean which is given by

$$V_{i\theta} = \frac{1}{n_i} \left(\sum |F_{i\theta}(x, y) - P_{i\theta}| \right) \quad (20)$$

For all $i_s \forall i \in 0 \dots 139$

Where n_i is the number of pixels in S_i and is the mean of pixel values of $F_{i\theta}(x, y)$ in sector S_i .

2.6 Classification and Decision

Hamming distance (HD) is calculated and used in classifying, if X and Y represent two binary patterns from iris image being verified and one in the database, HD is calculated by taking XOR of the two. It is the decision making parameter that was suggested by Dr. JG Daugman [4], mathematically, hamming distance (H.D) is given by

$$HD = \frac{\text{No_of_different_bits}}{\text{Total_No_of_bits}} \quad (21)$$

Matching algorithm

HD_array = {size (database)}

For $j=1$ to size (database) do

For $i = 1$ to 1120 do // for all 1120 bits in this work case

- XOR bit-by-bit code X_i with the code $Y(j)i$ in the database
- If the result of the XOR is (1), this mean the 2 bits are different, so count the number of ones
- Else don't count it and continue to the next bit
- Next i until reaching the final bit in IrisCode of position j .

Compute HD for j IrisCode

$$HD_j = \frac{\text{total_ones}}{1120}$$

$j = \text{size (database)}?$

If yes end

If No $j=j+1$

Decision

The smallest HD is selected from the array above then if is equal or less that the acceptable value, the corresponding individual is granted access, otherwise if HD is too large

2.7 Open system development

The details on coding can be requested through my email, this section shows the results and brief of the designed system, figure 14 bellow shows the main menu of the system designed

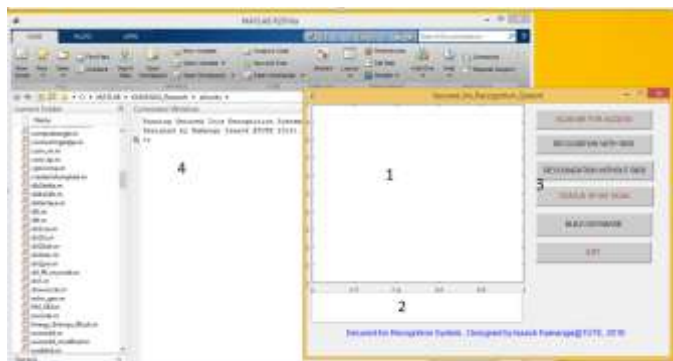


Figure 14: Designed system's main menu

Where by

- 1) Face preview area, the design is such that the algorithm zoom the detected individual face and then crop one eye for recognition, figure 3.16 shows the face preview of individual requesting scan to be granted an access.
- 2) Display 2 is used as an optional for viewing scanning status.
- 3) Control buttons, here all buttons are shown as it is for complete testing of the design but in real application, the individual shall be presented with only "scan me" control and shall be authenticated accordingly, display 2 is used as an optional for viewing scanning status. On the other hand, administrator shall be presented with "Build Database" control, to assist learning process of recognized personnel.
- 4) Main command window, this shows the current task being executed e.g features extraction of scanned eye, result of recognition process etc.



Figure 15: Designed system face preview and detected regions of interest

The system does what expected of not allowing further recognition stages from segmentation after an spoof attempt is detected, figure 16 show the result,

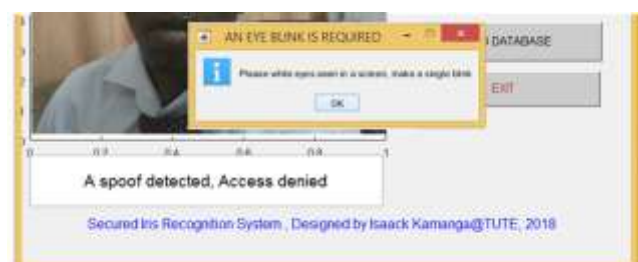


Figure 16: System reaction to spoof attempt

3. Experiment and Results Discussion

The performance of the secured iris recognition system as a whole is examined. Tests were carried out to find the best separation, so that the false match and false accept rate is minimized, in the event of spoof attempt and no spoof attempt scenario and to confirm that iris recognition can perform accurately as a biometric for recognition of individuals. As well as confirming that the system provides accurate recognition, experiments were also conducted in order to confirm the uniqueness of human iris patterns by reducing the number of degrees of freedom present in the iris template representation

3.1 Data set

When benchmarking an algorithm it is recommendable to use a standard test data set for researchers to be able to directly compare the results. While there are many databases in use currently, the choice of an appropriate database to be used should be made based on the task, in this work first testing was made on capability of the developed algorithm to detect eye blink, a suitable publicly available database from Zhejiang University, ZJU Eyeblink database and another publicly available database, the TalkingFace were used. Second testing was made on the capability of the system to detect any background variation on different picture frames, ZJU Eyeblink database were used and finally the testing on the accuracy of individuals recognition was done using ACASIA v3 database which is also publicly available



Figure 17: Samples from ZJU blinking database (the last line showing the upward orientation)

Table 1: Demography of blinking database

No. of Individuals	No. of Video clip	Face appearance	Total No. of blinks (TB)	Blinks detected (DB)	Blinks detected as no blink (MB)
20	1	Frontal	255	248	7
20	1	Frontal	255	248	7
20	1	Upward	255	215	40
20	1	Frontal	255	246	9

Accuracy of detection and error in detection are computed by equations (22) and (23) below respectively

$$Accuracy = \frac{DB}{TB} \times 100\% \quad (22)$$

$$Error = \frac{MB}{TB} \times 100\% \quad (23)$$

$$Accuracy = \frac{246}{255} \times 100\%$$

$$Accuracy = 96.47\%$$

$$Error = \frac{9}{255} \times 100\%$$

$$Error = 3.53\%$$

There are a number of parameters in the iris recognition system, and optimum values for these parameters were required in order to provide the best recognition rate. These parameters include; the radial and angular resolution, r and θ respectively, which give the number of data points for encoding each template.

4. Conclusion and Recommendation

Both industry and academia are focusing their efforts to make biometric devices more robust but every countermeasure can eventually be circumvented. Thus research and development efforts must be ongoing. This paper investigates eye blinks as aliveness detection against photo spoofing in face recognition and suggests the use of background subtraction and comparison as well as straight line border edge lines detection as the method for video and 3D-model spoofing attempt detection. The advantage of using eye blink-based method is a non-intrusion, no extra hardware requirement, and prominence of activity. To recognize the eye blink behavior, we do not need such a powerfully camera, camera as powerful as a webcam can accomplish the task. The testing found the algorithm developed to respond by 96.47% on the ZJU Eyeblick database.

References

- [1] J. G. Daugman, The importance of being random: Statistical principles of iris recognition, *Pattern Recognition*, vol. 36, pp. 279–291, 2003
- [2] Daugman JG., "High confidence Visual recognition of persons by a test of statistical independence," *IEEE Transaction on pattern analysis and machine Intelligence*, vol.5 no 11, pp.1148- 1161, 1993
- [3] Daugman, JG., " Probing the Uniqueness and Randomness of IrisCodes: Results from 200 Billion Iris Pair Comparisons", *IEEE*, Vol. 94, No. 11, November 2006.
- [4] Daugman, JG, "How iris recognition works", *IEEE Trans Circuits System and Video Technology*, vol. 14, pp. 1–17, 2003.
- [5] W. Kong and D. Zhang, "Accurate iris segmentation based on novel reflection and eyelash detection model", *Proceedings of 2001 International Symposium on Intelligent Multi-media, Video and Speech Processing*, Hong Kong, 2001
- [6] Wojciech Wojcikiewicz, "Hough Transform, Line Detection in Robot Soccer", *Coursework for Image Processing*. 14th March 2008
- [7] J. Borovička, "Circle Detection Using Hough Transforms Documentation". COMS30121 - Image Processing and Computer Vision, 2003.
- [8] T.Moriyama, T.Kanade, J.F.Cohn, J.Xiao, Z.Ambadar, J.Gao, H.Imamura, Automatic Recognition of Eye Blinking in Spontaneously Occurring Behavior. *ICPR'02*, 2002
- [9] Gang Pan, Lin Sun, Zhaohui Wu, Shihong Lao, "Eyeblick based Anti-Spoofing in Face Recognition from a Generic Web camera"
- [10] H. Rhody Chester F. "Hough Circle Transform", *Carlson Center for Imaging Science Rochester Institute of Technology* October 11, 2005.
- [11] <http://www.intechopen.com/>
- [12] <http://article.sapub.org/10.5923.j.scit.20120205.02.html> Retrieved on 4th September, 2017 1500hrs
- [13] Kristin Adair Nixon, Valerio Aimale, Robert K. Rowe, "spoof detection schemes", *Handbook of Biometrics*, Springer, 2007
- [14] Stephanie A. C. Schuckers, "Spoofing and Anti-spoofing measures". *Information Security Technical Report*, Vol 7, No. 4 (2002) 56-62
- [15] Wikipedia (ways of fighting iris spoofing)
- [16] <http://www.biometricupdate.com/201503/spoofing-iris-recognition-technology-with-pictures>
- [17] Divjak, M., Bischof, H.: Real-time video-based eye blink analysis for detection of low blink-rate during computer use. In: *First International Workshop on Tracking Humans for the Evaluation of their Motion in Image Sequences (THEMIS)*, pp. 99|107 (2008)
- [18] Fathi, Abdolhossein, and Fardin Abdali-Mohammadi. "Camera-based eye blinks pattern detection for intelligent mouse." *Signal, Image and Video Processing* 9.8 (2015): 1907- 1916.
- [19] Don't blink: Iris recognition for biometric identification. <http://www.sans.org/readingroom/whitepapers/authentication/dont-blink-iris-recognition>
- [20] Kamanga, Isaack, "An Adaptive Approach to Improve Canny Method for Edge Detection.", *International Journal of Science and Research (IJSR)* Volume 6 Issue 6, June 2017
- [21] Viola, P. and Jones, M. (2004). Robust real-time face detection. *IJCV*, 57(2):137–154. 6. Pan, Gang, Lin Shun, Zhaohui Wu, and Shihong Lao. " ZJU Eyeblick Database." *ZJU Eyeblick Database*. N.p., n.d. Web. 09 September 2017
- [22] Sanpachai, H and Settapong, M, M, "A study of Image Enhancement for Iris Recognition", *Journal of Industrial and Intelligent Information* Vol. 3, No. 1, March 2015
- [23] Ali A. Ibrahim, " iris recognition using Gabor filters", *AI – Taqani* , Vol.21, No. 1, 2008
- [24] R.Garg, B. Mitta, and S.Garg, "Histogram equalization techniques for image enhancement," *International Journal of Electronics & Communication Technology*, vol. 2, no. 1, pp. 107- 111, March 2011
- [25] "Android Studio Release Notes". *Android Developers Official Website*. June 8, 2017. Retrieved June 9, 2017
- [26] GUTCHES, D., M. T., COHEN-SOLAL, E., LYONS, D. and JAIN, A. K. 2001. A background model initialization algorithm for video surveillance. In *Eighth International Conference on Computer Vision*

- [27] KAEW TRA KUL PONG, P., AND BOWDEN, R. 2001. An improved adaptive background mixture model for real time tracking with shadow detection. In Proc. 2nd European Workshop on Advanced Video-Based Surveillance Systems
- [28] M C IVOR, A. 2000. Background subtraction techniques. In Proceedings of Image & Vision Computing New Zealand 2000 IVCNZ'00, Reveal Limited, Auckland, New Zealand.
- [29] STAUFFER, C., AND GRIMSON, W. 1999. Adaptive background mixture models for real time tracking. In Computer Vision and Pattern Recognition

Author Profile



Isaack Kamanga received the B.S. in Telecommunications Engineering from University of Dar Es Salaam in 2012, Tanzania, worked as Engineer in fields of RF, VSAT, Optic fiber network for 2 years, currently working as Tutorial assistant at Dar Es Salaam Institute of Technology (DIT), and doing masters degree in Signal and Information processing Engineering at Tianjin University of Technology and Education (TUTE), P.R China, with research base in computer vision.



Prof. Dening Jiang is an Associate professor at Tianjin University of Technology and Education (TUTE) with a research base in Image processing, embedded systems, cotemporary digital signal processing and design of optical crystal for THZ wave signal processing. He obtained his BSc, MSc. at Tianjin University of science and technology and PhD at Tianjin University